



**HAL**  
open science

# Interactions shape aquatic microbiome responses to Cu and Au nanoparticle treatments in wetland manipulation experiments

Zhao Wang, Christina Bergemann, Marie Simonin, Astrid Avellan, Phoebe Kiburi, Dana Hunt

► **To cite this version:**

Zhao Wang, Christina Bergemann, Marie Simonin, Astrid Avellan, Phoebe Kiburi, et al.. Interactions shape aquatic microbiome responses to Cu and Au nanoparticle treatments in wetland manipulation experiments. *Environmental Research*, 2024, 252, pp.118603. 10.1016/j.envres.2024.118603. hal-04579728

**HAL Id: hal-04579728**

**<https://hal.science/hal-04579728>**

Submitted on 18 May 2024

**HAL** is a multi-disciplinary open access archive for the deposit and dissemination of scientific research documents, whether they are published or not. The documents may come from teaching and research institutions in France or abroad, or from public or private research centers.

L'archive ouverte pluridisciplinaire **HAL**, est destinée au dépôt et à la diffusion de documents scientifiques de niveau recherche, publiés ou non, émanant des établissements d'enseignement et de recherche français ou étrangers, des laboratoires publics ou privés.

1 **Interactions shape aquatic microbiome responses to Cu and Au nanoparticle treatments in**  
2 **wetland manipulation experiments**

3

4 **Running title: Interactions mediate microbiome nanoparticle responses**

5

6 Zhao Wang<sup>1</sup>, Christina M. Bergemann<sup>2,3</sup>, Marie Simonin<sup>2,3,4</sup>, Astrid Avellan<sup>2,5,6</sup>, Phoebe Kiburi<sup>1</sup>,

7 Dana E. Hunt<sup>1,2\*</sup>

8 <sup>1</sup> Duke University Marine Laboratory, Beaufort NC USA

9 <sup>2</sup> Center for the Environmental Implications of Nanotechnology (CEINT), Duke University,  
10 Durham, North Carolina 27708, USA

11 <sup>3</sup> Biology Department, Duke University, Durham, North Carolina 27708, USA

12 <sup>4</sup> Present Address: University Angers, Institut Agro, INRAE, IRHS, SFR QUASAV, F-49000  
13 Angers, France

14 <sup>5</sup> Department of Civil and Environmental Engineering, Carnegie Mellon University, Pittsburgh,  
15 Pennsylvania 15289 USA

16 <sup>6</sup> Present Address: Géosciences Environnement Toulouse (GET), CNRS, Université de Toulouse,  
17 IRD, Toulouse, France.

18

19 \* Corresponding author

20

21

22

23

24

25

26 **Keywords: microbiome; nanoparticles; mesocosms; ecosystem complexity; biologically-**  
27 **mediated interactions**

28

29 **Corresponding Author Contact Information:**

30 135 Duke Marine Lab Rd

31 Beaufort NC 28516 USA

32 [dana.hunt@duke.edu](mailto:dana.hunt@duke.edu)

33 Phone: 252-646-9058

34 FAX: 252-504-7648

35 **Abstract**

36

37 In natural systems, organisms are embedded in complex networks where their physiology and  
38 community composition is shaped by both biotic and abiotic factors. Therefore, to assess the  
39 ecosystem-level effects of contaminants, we must pair complex, multi-trophic field studies with  
40 more targeted hypothesis-driven approaches to explore specific actors and mechanisms. Here, we  
41 examine aquatic microbiome responses to long-term additions of commercially- available  
42 metallic nanoparticles [copper-based (CuNPs) or gold (AuNPs)] and/or nutrients in complex,  
43 wetland mesocosms over 9 months, allowing for a full growth cycle of the aquatic plants. We  
44 found that both CuNPs and AuNPs (but not nutrient) treatments showed shifts in microbial  
45 communities and populations largely at the end of the experiment, as the aquatic plant  
46 community senesced. we examine aquatic microbiomes under **chronic** dosing of NPs and  
47 nutrients Simplified microbe-only or microbe + plant incubations revealed that direct effects of  
48 AuNPs on aquatic microbiomes can be buffered by plants (regardless of seasonal As mesocosms  
49 were dosed weekly, the absence of water column accumulation indicates the partitioning of both  
50 metals into other environmental compartments, mainly the flocc and aquatic plants  
51 photosynthetically-derived organic matter. Overall, this study identifies the potential for NP  
52 environmental impacts to be either suppressed by or propagated across trophic levels via the  
53 presence of primary producers, highlighting the importance of organismal interactions in  
54 mediating emerging contaminants' ecosystem-wide impacts.

55

56

57

58 **Funding**

59

60 This work was supported by the National Science Foundation (NSF) and the Environmental  
61 Protection Agency (EPA) under NSF Cooperative Agreement EF-0830093 and DBI-1266252,  
62 Center for the Environmental Implications of Nanotechnology (CEINT) and the National  
63 Science Foundation (ICER: 2033934, DEB: 2224819) to DEH. Any opinions, findings,  
64 conclusions or recommendations expressed in this material are those of the author(s) and do not  
65 necessarily reflect the views of the NSF or the EPA. This work has not been subjected to EPA  
66 review and no official endorsement should be inferred.

67

68

69

70

71

72

73

74

75

76

77

78

79

80

81 **Introduction**

82

83 Among emerging contaminants, engineered metallic nanoparticles (NPs) have received increased  
84 attention as their consumer applications have expanded (Saravanan et al., 2021). NPs' small size  
85 (1-100 nm) and large surface area: volume ratio generally increase their reactivity relative to  
86 their bulk counterparts (Auffan et al., 2009). The biological impacts of inorganic nanoparticles  
87 are generally attributed to the release of dissolution products or nano-specific effects due to their  
88 physical properties. For example, metallic NPs can disrupt cell membranes and generate  
89 oxidative stress, resulting in lipid and protein peroxidation and DNA damage (Clar et al., 2016;  
90 Maurer-Jones et al., 2013). Concerns about NP ecotoxicity have grown, as rates of anthropogenic  
91 nanoparticle deposition now rival those of natural NPs in some areas (Hochella et al., 2019).  
92 While most nanomaterial studies initially focused on model NPs, there is a growing interest in  
93 expanding our understanding of the ecosystem-level impacts of commercially-available NPs,  
94 which primarily enter the environment through disposal or application (Carley et al., 2020;  
95 Mitrano et al., 2015; Ward et al., 2019). In these commercial applications, NPs' advantages  
96 include lower substrate requirements; for example, while copper has been used as a pesticide for  
97 over a hundred years, newer copper-NP based biocides like Kocide® 3000 (Dupont) both  
98 enhance antimicrobial properties and reduce Cu usage (Giannousi et al., 2013; Kah et al., 2018).  
99 As biocides are commonly used in conjunction with other agrochemicals like fertilizers, these  
100 co-occurring contaminants could alter ecosystems with impacts distinct from either the fertilizer  
101 or pesticide alone (Kah, 2015).

102

103 However, it may be difficult to *a priori* predict the ecosystem outcomes of these NP-containing  
104 agrochemical mixtures because of (i) NP metastability which means their (bio)transformation  
105 and fate are dynamic, and differ from bulk counterparts (Avellan et al., 2020), or (ii) interactions  
106 between multiple contaminants that can lead to unexpected biological impacts (Brennan and  
107 Collins, 2015; Hagenbuch and Pinckney, 2012). For example, nutrients can attenuate  
108 contaminant toxicity directly by binding contaminants, or indirectly by increasing the organism's  
109 biomass or energy investment in detoxification (Aristi et al., 2016; Leflaive et al., 2015; Pieters  
110 et al., 2005; Skei et al., 2000). Conversely, nutrients can increase toxicity through enhanced  
111 contaminant uptake (Hu et al., 2013). As we cannot robustly predict ecosystem outcomes from  
112 short-term, laboratory studies, recent research has focused on environmentally realistic  
113 conditions including contaminant mixtures or co-occurring stressors in complex multi-trophic  
114 systems.

115

116 Microbes are a critical component of all ecosystems: with high diversity, short generation times  
117 and as critical mediators of biogeochemical cycles, the microbiome can be a sensitive and  
118 ecologically-important indicator of disturbance (Aylagas et al., 2017; Hunt and Ward, 2015).

119 Although early NP microbiome research focused on acute exposures in bacterial model systems  
120 (e.g. *Escherichia coli*), the field has shifted toward chronic exposures and whole community  
121 microbiome analyses. These community-level microbiome studies incorporate key, often  
122 uncultured organisms; account for different responses within microbiomes and incorporate  
123 modification of NP by other organisms or ecosystem components (Chae et al., 2014; Colman et  
124 al., 2014; Ward et al., 2019). Thus, there is a growing body of literature on how interactions with  
125 other organisms, and their associated biomacromolecules and ligands, can alter microbial

126 responses to toxicants through competition for resources, alteration of organic matter quantity  
127 and/or quality, or transformation and accumulation of contaminants (Bone et al., 2012; Ge et al.,  
128 2014).

129  
130 Here, to investigate how ecosystem complexity and co-occurring anthropogenic contaminants  
131 shape microbial responses to NPs, we examine aquatic microbiomes under chronic dosing of  
132 NPs and nutrients (N and P) in wetland mesocosms. We focus on two NPs: the commercially-  
133 available agricultural biocide Kocide® 3000 [containing  $\text{Cu}(\text{OH})_2$  NPs] and citrate-coated gold  
134 nanoparticles (AuNPs). While AuNPs were initially used primarily as a tracer of NP fate  
135 (Avellan et al., 2018), they have potential commercial applications in catalysts, sensors and  
136 medical treatments as well as potential ecotoxicity. Both these NP-based contaminants were  
137 chronically dosed into wetland mesocosms with either nanoparticles (CuNPs or AuNPs),  
138 nutrients, or both a single NP type and nutrients, over a 9-month period. Prior research on these  
139 mesocosms has revealed unexpected organismal responses (Perrotta et al., 2020), NP  
140 (bio)transformations (Avellan et al., 2020) and increased macroalgal blooms under chronic NP  
141 and nutrient dosing (Simonin et al., 2018a). However, it is still unclear how exposure to multiple  
142 stressors impacts aquatic microbial communities (Rillig et al., 2019). Further, as these  
143 mesocosms contain a complex food web including fish, snails, and plants, microbiome  
144 composition reflects both direct contaminant impacts and indirect effects mediated by  
145 interactions with other organisms (Hunt and Ward, 2015). To directly address the issue of  
146 ecosystem complexity, we employed a microcosm experiment (Bergemann et al., 2023) to  
147 address AuNP treatment effects in simplified communities composed of either only microbes or  
148 both microbes and the aquatic plant *Egeria densa*. Thus, this set of experiments focus on

149 identifying key environmental factors that mediate microbial responses to emerging pollutants in  
150 dynamic aquatic environments.

151

## 152 **Methods**

153

### 154 **Wetland mesocosm experiments**

155 Experiments were conducted at the Center of Environmental Implications of Nanotechnology  
156 (CEINT) mesocosm facility in the Duke University Forest (Durham, North Carolina, USA) from  
157 January 2016 - October 2016. Details about experimental set-up and monitoring were previously  
158 described (Lowry et al., 2012; Simonin et al., 2018a). Briefly, slantboard mesocosms (3.66 m  
159 long, 1.22 m wide and 0.8 m high) lined with a water-tight geotextile (0.45 mm reinforced  
160 polypropylene, Firestone Specialty Products, U.S.) were partially filled with sand, creating a  
161 permanently flooded zone (aquatic zone), a periodically flooded zone (transition zone), and a  
162 rarely flooded zone (upland zone). The mesocosms were filled with well water sourced at the site  
163 with an average starting water volume of 452 L; as the water level fluctuated over time with  
164 precipitation and evapotranspiration, therefore dosing is provided as weight rather than  
165 concentration. Organisms were introduced sequentially prior to starting the experiment in 2015,  
166 including the floating plant *Egeria densa*; aquatic snails *Physella acuta* and *Lymnaea* sp.; and the  
167 fish *Gambusia holbrooki* (eastern mosquitofish). An algal and zooplankton inoculum was added  
168 biweekly to reduce major divergences between mesocosms due to dispersal limitation and  
169 wetland plants were seeded in the transition zone.

170



171 Mesocosms were randomly assigned to one of six treatments (three replicates per treatment):  
172 control-ambient nutrient, control-nutrient enriched, AuNPs-ambient nutrient, AuNPs-nutrient  
173 enriched, Kocide (CuNPs)-ambient nutrient, and Kocide (CuNPs)-nutrient enriched. The  
174 synthesis and TEM characterization of citrate-stabilized AuNPs (average diameter:  $11.9 \pm 1.2$   
175 nm) and characterization of copper hydroxide NPs (average diameter:  $38.7 \pm 8.2$  nm) (CuNPs;  
176 Kocide 3000; DuPont, Wilmington, Delaware, USA) were described previously (Simonin et al.,  
177 2018a). Mesocosms dosed with AuNPs received a weekly dose of 19 mg Au, resulting in a total  
178 dose of 750 mg Au after 9 months. As Kocide is 27% Cu, CuNP mesocosms received an initial  
179 pulse of 93.7 mg of Cu and then a weekly dose of 9.5 mg of Cu, resulting in a total dose of 450  
180 mg Cu as Kocide per mesocosm after 9 months. Starting in September 2015, the nutrient-  
181 enriched treatments received 1 L of mesocosm water each week supplemented with 88 mg of N  
182 as  $\text{KNO}_3$  and 35 mg of P as  $\text{KH}_2\text{PO}_4$  to mimic agricultural run-off. This was a collaborative  
183 project and the nutrient amendment conditions were part of a complex experimental design that  
184 balanced the needs of many researchers, including preventing water column hypoxia.  
185  
186 Au and Cu concentrations in unfiltered surface water and other environmental metadata  
187 including temperature were collected as previously described (Avellan et al., 2020). To examine  
188 the microbial community, the aquatic zone was sampled immediately before dosing (D0), then 1  
189 and 7 days (D1, D7) after dosing, as well as after the first (T1), second (T2) and third (T3)  
190 quarters. At each timepoint, ~250 mL of water was collected from the near-surface (~0.25 m  
191 depth) by submerging sterile polypropylene bottles, and microbial biomass was collected from  
192 ~100-250 mL of water on 0.22  $\mu\text{m}$  Supor filters (Pall) via gentle vacuum filtration upon return to  
193 the lab. Samples were stored at  $-80$  °C until DNA extraction.

194

195 **Jar microcosm experiments**

196

197 In this experimental follow up to the outdoor mesocosms, simplified microcosms in one-quart  
198 acid-washed Ball® glass mason jars examined the impacts of ecosystem complexity and  
199 seasonal conditions on AuNP-dosed microbiomes, as described previously (Bergemann et al.,  
200 2023). Four treatments were chosen to compare with mesocosms mimicking both season (spring  
201 and early fall) and ecosystem complexity (microbes only or microbes + *Egeria*). Environmental  
202 Growth Chambers were set to match spring conditions (light: dark 12:12 hrs; irradiance  $481.95$   
203  $\pm 4.14$  lum ft<sup>-2</sup>; temperature 15 °C and 10°C in the light and dark periods, respectively) and  
204 early fall (15:9 hrs light: dark cycle; irradiance  $521.65 \pm 3.08$  lum ft<sup>-2</sup>; temperature 30 °C and 20  
205 °C in the light and dark periods, respectively). We note the “season” label differs between this  
206 paper and a prior publication (Bergemann et al., 2023). Both spring and fall conditions were  
207 assayed for two ecosystem complexities: microbes only and microbes + *Egeria densa*, with 6  
208 replicate jars for each condition. Each microcosm was filled with 100 g of washed Quickrete  
209 pool filter sand 700 mL of 0.25mm filtered water collected in July 2017 from a control  
210 mesocosm (described above) and 1 mL of 0.25 mm filtered local wetland water; filtration  
211 removed large organisms and debris to establish a microbiome. Macrophyte-containing  
212 microcosms also included five rinsed shoots of *E. densa* with a total wet weight of 6g. Weekly  
213 for 5 weeks, 143.3 µg of nitrogen (N) and 56.97 µg of phosphorus (P) were added to each  
214 microcosm as KNO<sub>3</sub> and KH<sub>2</sub>PO<sub>4</sub>. Each jar was capped with Parafilm® to allow the exchange of  
215 gases as well as light infiltration. After a week of acclimation, the AuNPs exposures began using

216 the same AuNP stock as the mesocosm experiment with 31.36  $\mu\text{g}$  of Au added per week for a  
217 total of 125.44  $\mu\text{g}$  over four weeks.

218

219 Water samples were collected to measure Au concentration and dissolved organic carbon (DOC).  
220 To measure Au concentration in the microcosms, 5 mL of water was collected weekly, acidified  
221 with  $\text{HNO}_3$  and  $\text{HCl}$ , then quantified using ICP-MS (Agilent 7700 and 7900). At the end of the  
222 experiment, 10 mL of GFF-filtered water was collected to measure dissolved organic carbon  
223 (DOC) using a TOC-VCPH Analyzer with a TNM-1 module (Shimadzu). At the end of the  
224 experiment, microbial biomass for community analysis was collected from 100 mL of water on  
225 0.22  $\mu\text{m}$  Supor filters (Pall) via gentle vacuum filtration. Samples were stored at  $-80^\circ\text{C}$  until  
226 DNA extraction.

227

### 228 **Nucleic acid extraction, library preparation and sequence analysis**

229

230 Genomic DNA for SSU rRNA gene libraries was extracted using the Gentra Puregene  
231 Yeast/Bacteria kit (QIAGEN) supplemented with bead beating (60 seconds; Biospec), cleaned  
232 using the Zymo *OneStep* PCR inhibitor removal kit and quantified using a Nanodrop ND-1000.  
233 515F-926R (V4-V5) 16S rRNA gene libraries were constructed using a dual-barcode sequencing  
234 approach (Needham et al., 2019; Parada et al., 2016). PCR reactions were performed in triplicate  
235 with 20  $\mu\text{l}$  reactions containing 20 ng template DNA,  $1\times$  Taq Buffer, 0.5  $\mu\text{M}$  of each primer, 200  
236  $\mu\text{M}$  of dNTPs, and 0.4 U of non-proofreading Econo Taq (Lucigen). The thermal cycling  
237 conditions were 2 min at  $95^\circ\text{C}$ , followed by 25 cycles of 1 min at  $95^\circ\text{C}$ , 1 min at  $50^\circ\text{C}$ , 30 sec at  
238  $72^\circ\text{C}$ , and a final extension at  $72^\circ\text{C}$  for 10 min. Triplicate PCR reactions were pooled and gel

239 purified (QIAquick, QIAGEN). Libraries were pooled at the same concentration, and the final  
240 pooled library concentration and purity verified by TapeStation (Agilent) and sequenced at the  
241 Duke Center for Genomic and Computational Biology using v2 2 x250 bp sequencing on the  
242 Illumina MiSeq.

243

244 Barcodes were removed and sequences were assigned to each sample using CASAVA (Illumina)  
245 and MacQIIME v1.9.1, sequences were then cleaned and clustered using USEARCH v.9.2  
246 (Edgar, 2013). Low quality sequence ends were trimmed at a Phred quality score (Q) of 30 using  
247 a 10 bp running window. Paired-end reads were merged if the overlap was at least 10 bp with no  
248 mismatches. Sequences with expected errors >1 and/or a length <400 bp were removed. Potential  
249 chimeras were filtered with uchime2 in USEARCH v.9.2. MED v2.1 was then used to resolve  
250 amplicon sequence variants (ASVs) (Eren et al., 2015), with a minimum unique sequence  
251 abundance of 20. The remaining 10,374 ASVs represented 7,368,537 reads, representing 89% of  
252 all reads. The taxonomies of representative ASVs were classified using MacQIIME v1.9.1 using  
253 RDP classifier v2.2 (Wang et al., 2007). Mitochondrial and chloroplast sequences were removed  
254 and the libraries were then sub-sampled to 8,074 reads per library. SSU rRNA library sequences  
255 were deposited as Bioproject PRJNA613470.

256

257 Bray-Curtis dissimilarities were visualized using non-metric multidimensional scaling (NMDS)  
258 ordination, and beta-diversity was analyzed by permutational multivariate ANOVA  
259 (PERMANOVA) using the adonis function in the *vegan* R package (Oksanen et al., 2015). ASV  
260 relative abundances >0.1%, with an added pseudo count of 1 to avoid excessive zeros inflating  
261 the model, were used to identify taxa with statistically significant effects of nanoparticles

262 (CuNPs or AuNPs), nutrients or interactions between factors using DESeq2 with a multifactor  
263 design (Love et al., 2014). Comparisons between environmental variables utilized the non-  
264 parametric Wilcoxon signed rank test, and significant differences were identified when  $p < 0.05$   
265 (Benjamini-Hochberg adjusted).

266

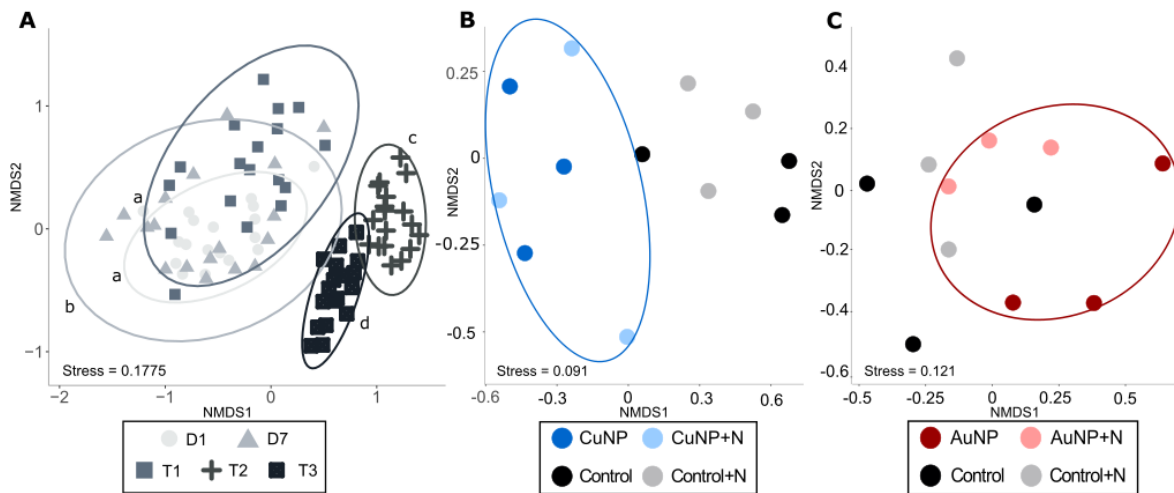
267

## 268 **Results and Discussion**

269

270 In order to characterize microbiome responses to NP-containing contaminant mixtures, here we  
271 initially focus on the aquatic compartment of wetland mesocosms exposed to factorial NP and  
272 nutrient treatments. In this experiment, CuNP treatments received a high initial dose (~94 mg of  
273 Cu as Kocide) to mimic a high load due to storm-driven transport and then weekly doses of  
274 CuNPs at concentrations approximating agricultural runoff (Simonin et al., 2018a). This  
275 approach led to high initial Cu in the water column that gradually declined over time (Figure S1).  
276 In contrast, AuNPs were applied at a steady rate and quickly sedimented out of the water  
277 column, resulting in aquatic gold concentrations that were slightly elevated over controls  
278 throughout the experiment (Figure S1). As mesocosms were dosed weekly, the absence of water  
279 column accumulation indicates the partitioning of both metals into other environmental  
280 compartments, mainly the floc and aquatic plants (Avellan et al., 2020). In order to understand  
281 how NPs and nutrient additions might impact aquatic microbial communities, we examined  
282 microbial community composition 1 day (D1) and 7 days (D7) after dosing initiation to identify  
283 initial treatment effects and after 3, 6, and 9 months (T1, T2 and T3) to investigate potential  
284 chronic or accumulation-driven microbiome impacts. While there were strong seasonal changes

285 in the microbial community (PERMANOVA,  $p < 0.05$ ; Figure 1A and Table S1), we did not  
286 identify a significant effect of nutrient addition alone or of NP-nutrient interactions on the  
287 microbiome (Figures 1, S2, S3 and Tables S2, S3). While nutrient addition previously alleviated  
288 Kocide inhibition of soil microbes (Simonin et al., 2018b), here we posit that most of the  
289 heterotrophic microbes are not nutrient-limited, thus low levels of added nitrogen and  
290 phosphorous did not significantly alter microbial community composition. However, prior  
291 research on these mesocosms found that nutrient-amended NP treatments intensified episodic  
292 macroalgal blooms, significantly altering competition between planktonic algae and floating  
293 plants and other environmental parameters (Simonin et al., 2018a). Somewhat surprisingly, the  
294 impact of nutrients on primary producers did not propagate to the non- eukaryotic, planktonic  
295 microbiome composition examined here; but higher nutrient concentrations or an increased  
296 number of mesocosm replicates might have revealed statistically-significant effects on the  
297 microbiome. As nutrient additions did not significantly alter the aquatic microbiome, we focused  
298 on the NP treatments by grouping the mesocosms with and without nutrient additions in  
299 subsequent analyses ( $n=6$ ). To identify potential nanoparticle treatment effects, we compared all  
300 NP-samples versus non-NP amended controls; significant community NP treatment effects were  
301 observed only in T3 for both Cu and Au NPs (Figures 1, S2, S3 and Tables S2, S3). Although the  
302 CuNP treatment microbial communities separated from controls on days 1 and 7 (Figure S2),  
303 samples violated the assumption of equal dispersion (betadisper,  $p < 0.05$ ), thus expected short-  
304 term CuNP treatment responses, potentially due to Cu toxicity, could not be evaluated  
305 statistically (Table S2).



306

307 **Figure 1. Mesocosm microbial community compositional changes over time and in response**  
 308 **to Cu and Au nanoparticles (NPs) and nutrient additions (+N).** (A) Non-metric  
 309 multidimensional scaling (NMDS) ordination computed based on Bray-Curtis dissimilarity for  
 310 16S rRNA gene libraries of all samples over time. Ellipses show 95% confidence intervals  
 311 around the mean. Samples with different letters “a”, “b”, “c” and “d” indicate significant  
 312 differences over time (by combining all mesocosms at each time point regardless of treatment;  
 313 pairwise PERMANOVA  $p < 0.05$ ). D1 and D7 indicate days relative to the initiation of NP  
 314 dosing. T1 (3-month), T2 (6-month) and T3 (9-month) represent quarterly samples. Panels (B)  
 315 and (C) show NMDS ordination based on Bray-Curtis dissimilarity for 16S rRNA gene libraries  
 316 at time points where the NP-treated mesocosms (combining NP and NP+N treatments)  
 317 statistically differed from the non-NP amended treatments (combining Control and Control +N).  
 318 The ellipses in (B) and (C) were manually drawn to highlight the effect of NPs on microbial  
 319 community composition. (B) Shows the significant microbiome impacts CuNP-treatment in the  
 320 third quarter (T3; PERMANOVA,  $p < 0.05$ ). (C) Shows the significant microbiome impacts of  
 321 AuNP-treatment in the third quarter (T3; PERMANOVA,  $p < 0.05$ ). “+N” indicates nutrient  
 322 additions, which did not significantly affect microbial community composition, nor interact with  
 323 CuNP or AuNP at any time point (PERMANOVA,  $p > 0.05$ ).

324

325 As neither metal accumulated in the aquatic compartment (Figure S1), the chronic (T3) aquatic  
 326 microbiome effects in both NP treatments were likely mediated by changes in the abundance or

327 physiology of other organisms (i.e. biological interactions), impacts of seasonality (e.g. effect of  
328 temperature, prevalence of sensitive organisms), or changes in the speciation and bioavailability  
329 of the metals (Avellan et al., 2020). Other potential explanations, such as gradual changes in the  
330 microbiome due to chronic exposure, were deemed unlikely due to rapid turnover in aquatic  
331 microbial populations. However, as treatments altered the balance between the macrophyte  
332 *Egeria* and planktonic algae in the aquatic zone (Simonin et al., 2018a), changes in the primary  
333 producer composition or metal-induced physiology could potentially alter the organic matter  
334 pool available to microbial communities. We were specifically interested in explaining the  
335 timing of the nanoparticle effect on microbiomes. While not a treatment effect, dissolved organic  
336 carbon (DOC) declined at the end of the experiment ( $\sim 5 \text{ mg L}^{-1}$  at T3 versus  $>10 \text{ mg L}^{-1}$  at other  
337 time points); as organic matter stabilizes and reduces the reactivity of NPs, lower organic matter  
338 levels could increase the toxicity of metallic NPs or their dissolution products (Aristi et al., 2016;  
339 Bone et al., 2012; Diegoli et al., 2008; Miao et al., 2009). These lower DOC levels in T3 are  
340 likely due to *Egeria* senescence (Avellan et al., 2020; Simonin et al., 2018a), potentially  
341 coupling ecotoxicity with plant growth stage. In addition to complexation with the nanoparticles  
342 directly, labile DOC produced by actively-growing primary producers could alleviate NP-  
343 toxicity by providing increased resources that allow microbial investment in detoxification etc.  
344 In short, for this complex wetland experiment, we predict that the effect of NPs and their  
345 transformation products on the water column microbial community are potentially predominately  
346 indirect impacts mediated by complex ecosystem interactions.

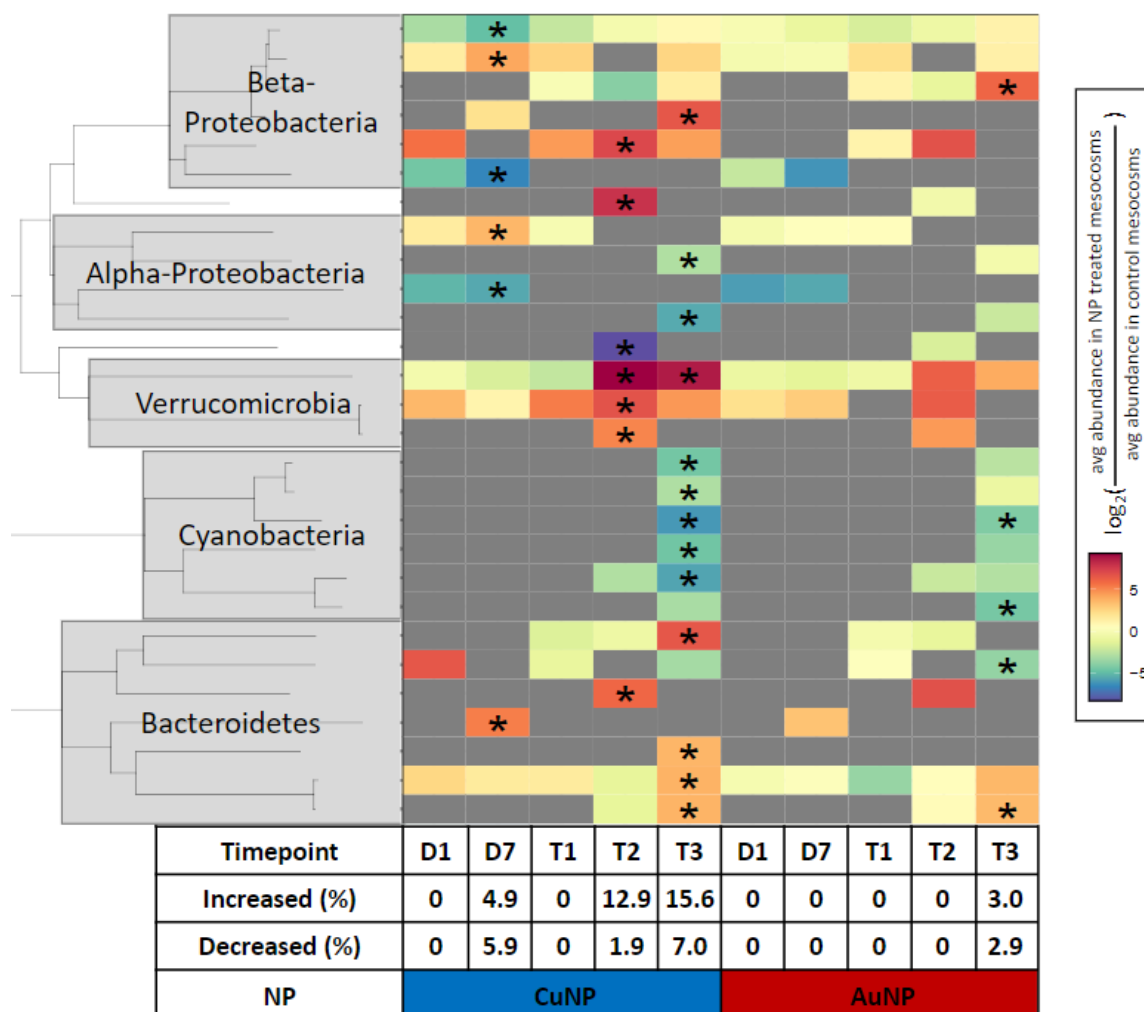
347

348 In order to gain greater insight into potential NP and nutrient effects on specific taxa, we  
349 examined population-level treatment responses using 16S rRNA gene amplicon sequence



350 variants (ASVs). Again, a two-factor design was applied to examine the impacts of  
351 nanoparticles, nutrient additions and interactions between these two factors. For example, the  
352 effect of the CuNP treatment was identified by comparing all Kocide-treated mesocosms versus  
353 the mesocosms without nanoparticles, regardless of nutrient addition (n = 6). As there were not  
354 significant differences between ambient and nutrient-amended treatments (Figures S4, S5), we  
355 again focus on nanoparticle treatments. At the population level, CuNP treatments showed  
356 significant effects on day 7 as well as at the T2 and T3 time points (Figure 2; Table S4). At the  
357 beginning of the experiment (D7), taxa comprising 5.9% of the community significantly declined  
358 versus 4.9% which increased in CuNP treatments compared to controls (Figure 2), suggesting a  
359 balance between toxicity effects and microbes which benefit from reduced competition or  
360 additional resources released by dying cells. In contrast, at later time points, a larger percentage  
361 of taxa significantly increased (12.9%, 15.6%) versus declined (1.9%, 7.0 %) of the CuNP-  
362 treated community in T2 and T3, respectively, suggesting that responsive phylotypes do not  
363 reflect environmental toxicity but also potentially include taxa which benefit from new niches or  
364 altered physiology in the NP- treatments (Figure 2). We considered a number of potential  
365 explanations for the observed Cu-treatment results including copper toxicity, Cu's role as a  
366 micronutrient that could stimulate growth, and ecosystem-level impacts including shifts in  
367 environmental resources. Treatment-responsive taxa were spread throughout the phylogenetic  
368 tree (Figure 2); however, some trends emerged which provide insight into potential mechanisms.  
369 Pertaining to the toxicity hypothesis, in T3 CuNP mesocosms, several cyanobacterial ASVs  
370 decreased (Table S4); these declines in cyanobacteria are consistent with either Cu toxicity or  
371 changes in the balance of primary producers, as observed previously (Simonin et al., 2018a), but  
372 by themselves are not conclusive. Second, we examined the potential for copper to act as a key

373 micronutrient (Clar et al., 2016; Jamers et al., 2013). As aquatic Cu concentrations are >10x  
374 limiting concentrations even in non-CuNP treatments (Posacka et al., 2019), population increases  
375 in CuNP-treatments are unlikely to reflect alleviation of Cu limitation. Finally, we examined the  
376 evidence for ecosystem-level changes in the system; in addition to declines in cyanobacterial  
377 relative abundance, in T2 CuNP treatments a number of Verrucomicrobia ASVs increased;  
378 Verrucomicrobia are known polysaccharide degraders and may reflect increased environmental  
379 availability of these compounds (He et al., 2017). Notably, these results contrast with previous  
380 chronic AgNP treatment mesocosms (Ward et al., 2019), where similar responsive taxa were not  
381 observed in both initial and long term exposure time points; the results in this study suggest  
382 either strong microbiome seasonality (Figure 1) or different factors governing microbial  
383 responses across the time course of the experiment. Thus, we conclude that chronic dosing of  
384 CuNPs yields a complicated response, with microbial populations potentially affected by CuNP  
385 treatments both directly (e.g. toxicity) and indirectly (e.g. via interactions with CuNP-responsive  
386 ecosystem components), as evidenced by microbial populations that increased as well as  
387 decreased in abundance. Compared to CuNP treatments, fewer taxa significantly increased or  
388 decreased at any time point in AuNP treatment mesocosms (Figure 2). All 5 AuNP treatment-  
389 responsive taxa were in T3; yet there was not an apparent phylogenetic signal (i.e. no clustering  
390 of responsive taxa in the phylogenetic tree) and responsive taxa both increased and decreased in  
391 relative abundance (Figure 2). In summary, population-level analysis shows that compared to  
392 AuNPs, CuNP treatment caused more widespread impacts across both time and microbial taxa,  
393 with AuNP treatment resulting in microbial community shifts relative to controls only at the end  
394 of the experiment, through an unknown mechanism.



395

396 **Figure 2. Mesocosm amplicon sequence variants (ASVs) that significantly respond to CuNP**  
 397 **or AuNP treatments.** Log<sub>2</sub> fold change of each ASV was calculated as

398  $\log_2\left(\frac{\text{avg abundance in NP treated mesocosms}}{\text{avg abundance in control mesocosms}}\right)$ . NP treated mesocosms include NP only and NP-

399 nutrient enriched mesocosms (n=6), and control mesocosms include both ambient control and  
 400 control + Nutrient addition mesocosms (n=6), as nutrients did not show any significant

401 individual or interactive effect with NPs on microbial community composition. ASVs are shown  
 402 in the plot if: (1) they are identified as significantly responding to CuNPs or AuNPs at any time

403 point using DESeq2 (Asterisks indicate the taxa relative abundance was significantly different  
 404 that controls  $p < 0.05$ ); and (2) ASV relative abundance exceeds the threshold of 0.2% at the

405 corresponding time point. Gray shading indicates that the ASV does not exceed the 0.2%

406 abundance threshold at that time point. ASVs are organized by a maximum likelihood

407 phylogenetic tree with major phyla labelled. Underneath the heatmap, the total relative

408 abundance of ASVs that significantly increased in the NP- treated mesocosms or declined in the  
409 control mesocosms are labeled with Increased (%) and Decreased (%).

410

### 411 **Microcosm experiments to explore ecosystem complexity in microbiome responses to NP**

412

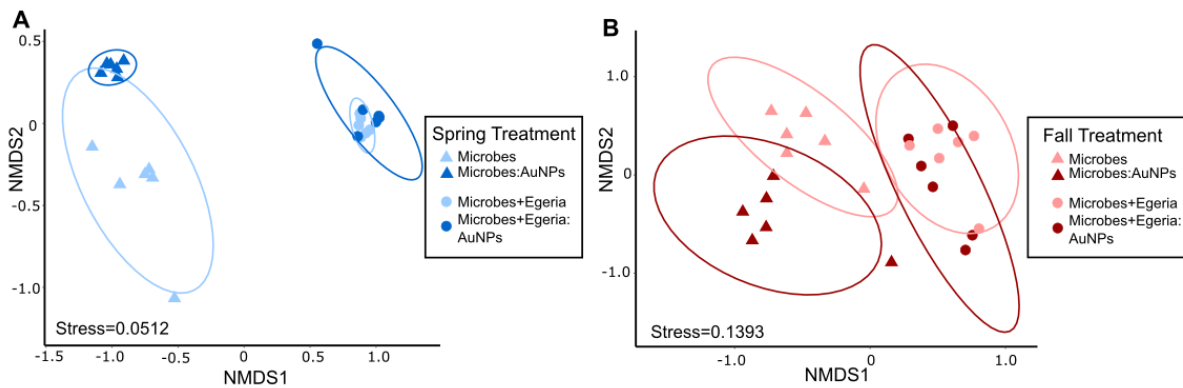
413 The question remains why T3 (fall) samples exhibited microbiome responses in AuNP and  
414 CuNP treatments, with the prediction that environmental factors rather than accumulation drives  
415 this response. We specifically focus on AuNP treatments, as elemental gold was historically  
416 taken as an inert tracer not toxic to microbes (Ahmad et al., 2013; Zhang et al., 2015), although  
417 recent examples of microbial toxicity have been noted in the literature (Sathiyaraj et al., 2021)..  
418 While the mechanisms of AuNP microbiome responses are unclear, they may include AuNP  
419 antimicrobial activity of either the NPs (Sathiyaraj et al., 2021) or their environmental  
420 transformation products including potentially-toxic gold ions or gold-containing compounds  
421 (Avellan et al., 2018). Moreover, the fact that AuNPs mesocosms exhibited a microbiome  
422 response at a single time point suggests a role for ecosystem interactions (Gräf et al., 2023),  
423 which we sought to test here through guided experimentation. In addition to direct toxicity,  
424 microbial community shifts could be explained by multi-stressor effects (e.g. warmer water  
425 temperatures in fall samples) or indirect effects through interactions with other AuNP-treatment  
426 sensitive organisms (Hunt and Ward, 2015; Wang et al., 2021). To differentiate among the  
427 mechanisms behind AuNP aquatic microbiome responses and to remove co-occurring changes  
428 with season (e.g. plant growth stage), we specifically tested the impact of season (spring or fall;  
429 temperature and light incubations) and ecosystem complexity (presence of primary producers)  
430 using simplified, month-long jar microcosms. Compared to the mesocosms, microcosms had  
431 reduced organismal complexity: microbes alone or microbes incubated with the aquatic plant

432 *Egeria*, the biomass-dominant primary producer in the aquatic compartment of the mesocosms,  
433 which provides heterotrophic bacteria with carbon, competes with microbial primary producers  
434 and alters water quality parameters (Figure S6). The month-long duration enables observation of  
435 microbiome shifts with seasonal incubation conditions and/or AuNP treatment, without the long-  
436 term accumulation effects that occurred over 9 months in the mesocosms. Microcosm conditions  
437 were set to match either the beginning (spring: D1, D7) or end of the experiment (fall: T3), when  
438 a significant AuNP microbiome treatment effect was observed.

439

440 In the microcosm experiment, we observed a strong season-treatment effect (Figure S7),  
441 consistent with the known impact of temperature on aquatic microbial communities (Wang et al.,  
442 2021; Ward et al., 2017) (Figure 3). However, contrary to our initial hypothesis of season-related  
443 interactions with AuNPs, for both spring and fall regimes, AuNP treatment influenced  
444 microbiome composition in the microbe-only but not in the microbiome + *Egeria* microcosms  
445 (for a given ecosystem complexity and season, microbiomes were compared with or without  
446 AuNP treatment: PERMANOVA,  $p < 0.05$ ; Figure 3). Thus, the presence of *Egeria* buffers the  
447 AuNP-treatment effect on microbes. Similarly, wetland plants were shown to mitigate the  
448 impacts of AgNPs on microbially-mediated biogeochemical cycles (He et al., 2022) and toxicity  
449 effects on juvenile fish (Bone et al., 2012), suggesting a more general role for primary producers  
450 in mediating NP toxicity. Consistent with these community-level results, more AuNP treatment-  
451 responsive taxa were identified in microbe-only (37) vs. microbes with *Egeria* treatments (1),  
452 (Figure S8). While AuNPs were initially predicted to exhibit minimal toxicity (Zhang et al.,  
453 2015), researchers have observed AuNP toxicity in microbial cultures (Ahmad et al., 2013;  
454 Hernández-Sierra et al., 2008) and Au bound to ligands (e.g. cyanide, hydroxyl and thiol) has

455 unknown microbial effects (Avellan et al., 2020; Avellan et al., 2018). Responsive taxa in the  
456 microcosm experiments included a number of shifts (both positive and negative) in the relative  
457 abundance of Bacteroidetes, potentially reflecting replacement of AuNP-treatment-sensitive taxa  
458 with resistant taxa that filled similar ecological niches (Figure S8). Thus, we examined other  
459 microcosm parameters to identify potential mechanisms for *Egeria*'s mediation of AuNP's  
460 microbiome impacts.  
461

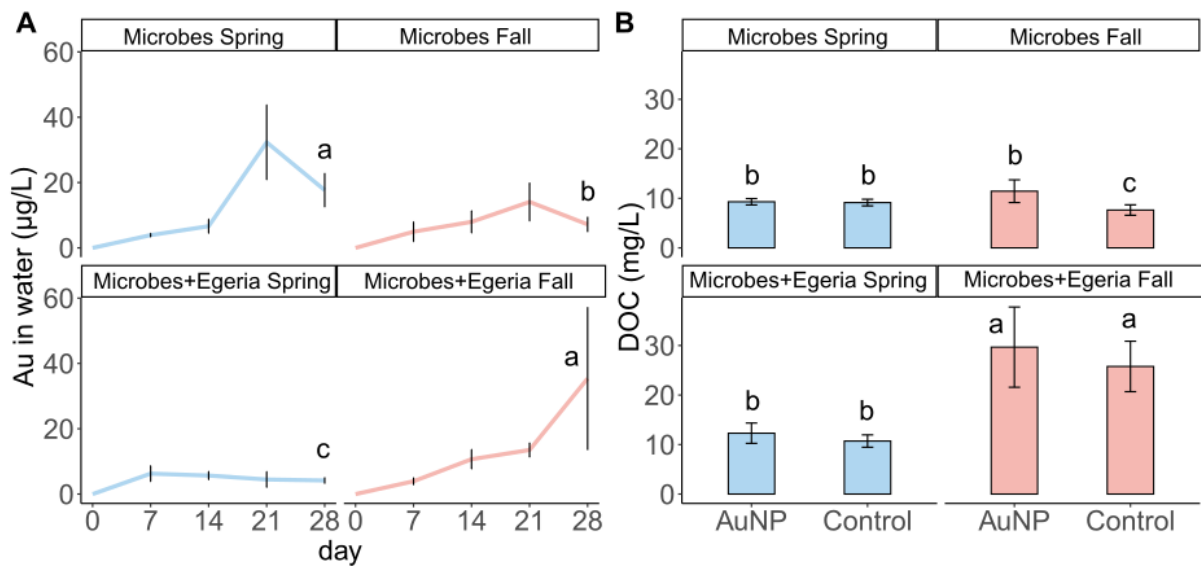


462  
463 **Figure 3. Microcosm microbial community changes (16S rRNA gene libraries) with gold**  
464 **nanoparticle conditions for different seasonal conditions and ecosystem complexity.** Jar  
465 microcosm microbiomes at the end of the experiment are shown as non-metric multidimensional  
466 scaling (NMDS) ordination based on Bray-Curtis dissimilarity. (A) Spring treatment conditions:  
467 average 12.5 °C, light:dark: 12:12 hours (B) Fall conditions: average 26.25 °C, light:dark: 15:9  
468 hours Ellipses (95% confidence intervals around the mean) show significant effects of AuNP  
469 treatment for a given seasonal treatment in the Microbe-only microcosms (PERMANOVA,  $p <$   
470 0.05). Triangles indicate microcosms with microbes only and circles those containing both  
471 microbes and the plant *Egeria densa*.  
472

473 Although AuNP treatments with *Egeria* did not exhibit shifts in microbiome composition in  
474 either season, water column parameters suggest *Egeria* has different effects on the AuNPs: in

475 spring, removal of gold from the water column and in fall stabilization and inactivation of water  
476 column gold through enhanced DOC concentrations (Glenn and Klaine, 2013). In the spring  
477 AuNP treatment microcosms, aquatic gold concentrations are significantly higher in the microbe-  
478 only condition (Figure 4A,  $p < 0.05$  Wilcoxon signed-rank test), and more gold accumulated in  
479 the *Egeria* (Microbe+ *Egeria* treatment) (Bergemann et al., 2023). In contrast, under fall  
480 conditions, water column gold was significantly higher (mean  $\sim 40 \mu\text{g L}^{-1}$ ) in the microbe +  
481 *Egeria* AuNP treatment than in the microbe-only treatment ( $\sim 10 \mu\text{g L}^{-1}$ , Figure 4A,  $p < 0.05$   
482 Wilcoxon signed rank test). This higher aquatic gold concentrations in the fall microbe + *Egeria*  
483 AuNP treatment could be explained by high *Egeria*-produced dissolved organic carbon (DOC)  
484 concentrations which stabilized aquatic Au and potentially reduced its toxicity (Figure 4B;  
485  $p < 0.05$  Wilcoxon signed rank test) (Aristi et al., 2016; Diegoli et al., 2008; Glenn and Klaine,  
486 2013; Miao et al., 2009). As the DOC concentration is elevated in *Egeria*-containing AuNP and  
487 Control treatments (Figure 4B), DOC levels are due to “fall” conditions rather than the AuNP  
488 treatment. Although we cannot definitively assign a mechanism, these results complement the  
489 field mesocosm’s conclusions that microbe-only studies may not readily translate to complex  
490 ecosystems, where interactions with other organisms (and environmental factors) mediate  
491 contaminant microbiome responses in complex and unpredicted ways. Overall, these combined  
492 experiments suggest that growing aquatic plants attenuates NP-toxicity; however, this protective  
493 effect is lost during *Egeria* senescence with the accompanying decline in aquatic DOC (as  
494 observed in the mesocosm experiment).

495



496

497 **Figure 4. Microcosm gold and dissolved organic carbon (DOC) colonized by either**  
 498 **microbes or microbes + *Egeria* incubated under spring and fall conditions.** (A) Total gold in  
 499 the water column over the 28-day incubation for AuNP treatment microcosms. Means on day 28  
 500 labeled with the same letter are not significantly different (Wilcoxon ranked sum test,  $p < 0.05$ ).  
 501 Error bars show one standard deviation. (B) Microcosm DOC concentrations on day 28 labeled  
 502 with the same letter are not significantly different (Wilcoxon ranked sum test,  $p < 0.05$ ). Error  
 503 bars show one standard deviation. Seasonal comparisons between spring (avg. 12.5 °C,  
 504 light:dark; 12:12 hours) and fall (avg. 26.25 °C, light:dark; 15:9 hours) treatments.

505

506

## 507 Conclusions

508

509 In these set of two linked experiments, we found that CuNPs and AuNPs treatments can exert  
 510 significant effects on aquatic microbial communities, but that microbiome responses are likely a  
 511 combination of direct effects as well as interactions with other ecosystem components. While  
 512 NPs can generate broad ecosystem-level effects either as synthesized or as transformation  
 513 products, as well as indirect effects mediated by interactions with other organisms (Hunt and



514 Ward, 2015), the impacts of nanoparticles are strongly mediated by environmental complexity.  
515 Here, we speculate that, compared to other taxa, primary producers have the potential to either  
516 suppress or propagate the effects of contaminants to other trophic levels due to their position at  
517 the base of the food web and biomass dominance in many ecosystems (Ge et al., 2014;  
518 Slaveykova, 2022). This research suggests that rather than requiring full-ecosystem complexity,  
519 simplified microcosms containing primary producers may allow greater insights into the impacts  
520 of nanoparticles and other contaminants on microbiomes. Thus, by focusing on critical  
521 ecosystem components, we can better understand the processes by which contaminants transform  
522 and are transformed by ecosystems.

523

#### 524 **Acknowledgements**

525 We acknowledge contributions of the entire CEINT mesocosm team to this research, especially  
526 the leadership of Emily Bernhardt.

527

#### 528 **CRedit Statement**

529 **Zhao Wang:** Data curation, Formal analysis, Investigation, Visualization, Writing-original draft

530 **Christina M. Bergemann:** Data curation, Investigation, Writing- review and editing

531 **Marie Simonin:** Data curation, Investigation, Writing- review and editing

532 **Astrid Avellan:** Data curation, Investigation, Writing- review and editing

533 **Phoebe Kiburi:** Investigation

534 **Dana E. Hunt:** Formal analysis, Resources, Visualization, Writing-original draft

535

536

537 **References**

538

- 539 Ahmad, T., et al., 2013. Antifungal activity of gold nanoparticles prepared by solvothermal  
540 method. *Materials Research Bulletin*. 48, 12-20.
- 541 Aristi, I., et al., 2016. Nutrients versus emerging contaminants—or a dynamic match between  
542 subsidy and stress effects on stream biofilms. *Environmental Pollution*. 212, 208-215.
- 543 Auffan, M., et al., 2009. Towards a definition of inorganic nanoparticles from an environmental,  
544 health and safety perspective. *Nature Nanotechnology*. 4, 634-641.
- 545 Avellan, A., et al., 2020. Differential Reactivity of Copper- and Gold-Based Nanomaterials  
546 Controls Their Seasonal Biogeochemical Cycling and Fate in a Freshwater Wetland  
547 Mesocosm. *Environmental Science & Technology*. 54, 1533-1544.
- 548 Avellan, A., et al., 2018. Gold nanoparticle biodissolution by a freshwater macrophyte and its  
549 associated microbiome. *Nature Nanotechnology*. 13, 1072-1077.
- 550 Aylagas, E., et al., 2017. A bacterial community-based index to assess the ecological status of  
551 estuarine and coastal environments. *Marine Pollution Bulletin*. 114, 679-688.
- 552 Bergemann, C. M., et al., 2023. Seasonal Differences and Grazing Pressure Alter the Fate of  
553 Gold Nanoparticles in a Microcosm Experiment. *Environmental Science & Technology*.  
554 57, 13970-13979.
- 555 Bone, A. J., et al., 2012. Biotic and abiotic interactions in aquatic microcosms determine fate  
556 and toxicity of Ag nanoparticles: part 2—toxicity and Ag speciation. *Environmental  
557 Science & Technology*. 46, 6925-6933.
- 558 Brennan, G., Collins, S., 2015. Growth responses of a green alga to multiple environmental  
559 drivers. *Nature Climate Change*. 5, 892-897.
- 560 Carley, L. N., et al., 2020. Long-Term Effects of Copper Nanopesticides on Soil and Sediment  
561 Community Diversity in Two Outdoor Mesocosm Experiments. *Environmental Science &  
562 Technology*. 54, 8878-8889.
- 563 Chae, S.-R., et al., 2014. Aging of fullerene C<sub>60</sub> nanoparticle suspensions in the presence of  
564 microbes. *Water Research*. 65, 282-289.
- 565 Clar, J. G., et al., 2016. Copper Nanoparticle Induced Cytotoxicity to Nitrifying Bacteria in  
566 Wastewater Treatment: A Mechanistic Copper Speciation Study by X-ray Absorption  
567 Spectroscopy. *Environmental Science & Technology*. 50, 9105-9113.
- 568 Colman, B. P., et al., 2014. Emerging Contaminant or an Old Toxin in Disguise? Silver  
569 Nanoparticle Impacts on Ecosystems. *Environmental Science & Technology*. 48, 5229-  
570 5236.
- 571 Diegoli, S., et al., 2008. Interaction between manufactured gold nanoparticles and naturally  
572 occurring organic macromolecules. *Science of the Total Environment*. 402, 51-61.
- 573 Edgar, R. C., 2013. UPARSE: highly accurate OTU sequences from microbial amplicon reads.  
574 *Nature Methods*. 10, 996-998.
- 575 Eren, A. M., et al., 2015. Minimum entropy decomposition: Unsupervised oligotyping for  
576 sensitive partitioning of high-throughput marker gene sequences. *The ISME Journal*. 9,  
577 968-979.

578 Ge, Y., et al., 2014. Soybean plants modify metal oxide nanoparticle effects on soil bacterial  
579 communities. *Environmental Science & Technology*. 48, 13489-13496.

580 Giannousi, K., et al., 2013. Synthesis, characterization and evaluation of copper based  
581 nanoparticles as agrochemicals against *Phytophthora infestans*. *RSC advances*. 3, 21743-  
582 21752.

583 Glenn, J. B., Klaine, S. J., 2013. Abiotic and biotic factors that influence the bioavailability of gold  
584 nanoparticles to aquatic macrophytes. *Environmental Science & Technology*. 47, 10223-  
585 10230.

586 Gräf, T., et al., 2023. Biotic and Abiotic Interactions in Freshwater Mesocosms Determine Fate  
587 and Toxicity of CuO Nanoparticles. *Environmental Science & Technology*. 57, 12376-  
588 12387.

589 Hagenbuch, I. M., Pinckney, J. L., 2012. Toxic effect of the combined antibiotics ciprofloxacin,  
590 lincomycin, and tylosin on two species of marine diatoms. *Water Research*. 46, 5028-  
591 5036.

592 He, G., et al., 2022. Aquatic macrophytes mitigate the short-term negative effects of silver  
593 nanoparticles on denitrification and greenhouse gas emissions in riparian soils.  
594 *Environmental Pollution*. 293, 118611.

595 He, S., et al., 2017. Ecophysiology of freshwater Verrucomicrobia inferred from metagenome-  
596 assembled genomes. *Mosphere*. 2, e00277-17.

597 Hernández-Sierra, J. F., et al., 2008. The antimicrobial sensitivity of *Streptococcus mutans* to  
598 nanoparticles of silver, zinc oxide, and gold. *Nanomedicine: Nanotechnology, Biology  
599 and Medicine*. 4, 237-240.

600 Hochella, M. F., et al., 2019. Natural, incidental, and engineered nanomaterials and their  
601 impacts on the Earth system. *Science*. 363, eaau8299.

602 Hu, Y., et al., 2013. Nitrate nutrition enhances nickel accumulation and toxicity in *Arabidopsis*  
603 plants. *Plant and Soil*. 371, 105-115.

604 Hunt, D. E., Ward, C. S., A network-based approach to disturbance transmission through  
605 microbial interactions. *Frontiers in Microbiology*, Vol. 6, 2015, pp. 1182.

606 Jamers, A., et al., 2013. Copper toxicity in the microalga *Chlamydomonas reinhardtii*: an  
607 integrated approach. *Biometals*. 26, 731-740.

608 Kah, M., 2015. Nanopesticides and nanofertilizers: emerging contaminants or opportunities for  
609 risk mitigation? *Frontiers in Chemistry*. 3, 64.

610 Kah, M., et al., 2018. A critical evaluation of nanopesticides and nanofertilizers against their  
611 conventional analogues. *Nature Nanotechnology*. 13, 677-684.

612 Leflaive, J., et al., 2015. Community structure and nutrient level control the tolerance of  
613 autotrophic biofilm to silver contamination. *Environmental Science and Pollution  
614 Research*. 22, 13739-13752.

615 Love, M. I., et al., 2014. Moderated estimation of fold change and dispersion for RNA-seq data  
616 with DESeq2. *Genome Biology*. 15, 1.

617 Lowry, G. V., et al., 2012. Long-term transformation and fate of manufactured Ag nanoparticles  
618 in a simulated large scale freshwater emergent wetland. *Environmental Science &  
619 Technology*. 46, 7027-7036.

620 Maurer-Jones, M. A., et al., 2013. Toxicity of engineered nanoparticles in the environment.  
621 *Analytical Chemistry*. 85, 3036-3049.

622 Miao, A.-J., et al., 2009. The algal toxicity of silver engineered nanoparticles and detoxification  
623 by exopolymeric substances. *Environmental Pollution*. 157, 3034-3041.

624 Mitrano, D. M., et al., 2015. Review of nanomaterial aging and transformations through the life  
625 cycle of nano-enhanced products. *Environment International*. 77, 132-147.

626 Needham, D., et al., 2019. Fuhrman Lab 515F-926R 16S and 18S rRNA Gene Sequencing  
627 Protocol V.2. protocols.io.

628 Oksanen, J., et al., 2015. Package 'vegan'. *Community ecology package*, version. 2.

629 Parada, A. E., et al., 2016. Every base matters: assessing small subunit rRNA primers for marine  
630 microbiomes with mock communities, time series and global field samples.  
631 *Environmental Microbiology*. 18, 1403-1414.

632 Perrotta, B. G., et al., 2020. Copper and Gold Nanoparticles Increase Nutrient Excretion Rates of  
633 Primary Consumers. *Environmental Science & Technology*. 54, 10170-10180.

634 Pieters, B. J., et al., 2005. Influence of food limitation on the effects of fenvalerate pulse  
635 exposure on the life history and population growth rate of *Daphnia magna*.  
636 *Environmental Toxicology and Chemistry*. 24, 2254-2259.

637 Posacka, A. M., et al., 2019. Effects of Copper Availability on the Physiology of Marine  
638 Heterotrophic Bacteria. *Frontiers in Marine Science*. 5.

639 Rillig, M. C., et al., 2019. The role of multiple global change factors in driving soil functions and  
640 microbial biodiversity. *Science*. 366, 886-890.

641 Saravanan, A., et al., 2021. A review on biosynthesis of metal nanoparticles and its  
642 environmental applications. *Chemosphere*. 264, 128580.

643 Sathiyaraj, S., et al., 2021. Biosynthesis, characterization, and antibacterial activity of gold  
644 nanoparticles. *Journal of Infection and Public Health*. 14, 1842-1847.

645 Simonin, M., et al., 2018a. Engineered nanoparticles interact with nutrients to intensify  
646 eutrophication in a wetland ecosystem experiment. *Ecological Applications*. 86, 1435-  
647 1449.

648 Simonin, M., et al., 2018b. Plant and microbial responses to repeated  $\text{Cu}(\text{OH})_2$  nanopesticide  
649 exposures under different fertilization levels in an agro-ecosystem. *Frontiers in*  
650 *Microbiology*. 9, 1769.

651 Skei, J., et al., 2000. Eutrophication and contaminants in aquatic ecosystems. *AMBIO: A Journal*  
652 *of the Human Environment*. 29, 184-194.

653 Slaveykova, V. I., 2022. Phytoplankton Controls on the Transformations of Metal-containing  
654 Nanoparticles in an Aquatic Environment. *Environmental Nanopollutants*. 9, 113.

655 Wang, Q., et al., 2007. Naive Bayesian classifier for rapid assignment of rRNA sequences into  
656 the new bacterial taxonomy. *Applied and Environmental Microbiology*. 73, 5261.

657 Wang, Z., et al., 2021. Environmental stability impacts the differential sensitivity of marine  
658 microbiomes to increases in temperature and acidity. *The ISME Journal*. 15, 19-28.

659 Ward, C. S., et al., 2019. Conserved Microbial Toxicity Responses for Acute and Chronic Silver  
660 Nanoparticle Treatments in Wetland Mesocosms. *Environmental Science & Technology*.  
661 53, 3268-3276.

662 Ward, C. S., et al., 2017. Annual community patterns are driven by seasonal switching between  
663 closely related marine bacteria. *The ISME Journal*. 11, 1412-1422.

664 Zhang, Y., et al., 2015. Antimicrobial activity of gold nanoparticles and ionic gold. *Journal of*  
665 *Environmental Science and Health, Part C*. 33, 286-327.

